Type I interferon susceptibility distinguishes SARS-CoV-2 from SARS-CoV
— Source link ⬈

Kumari G. Lokugamage, Adam Hage, Maren de Vries, Ana M. Valero-Jimenez ...+4 more authors

Institutions: University of Texas Medical Branch, New York University

Topics: Coronavirus, Viral replication, Interferon and Influenza A virus

Related papers:

- SARS-CoV-2 sensitive to type I interferon pretreatment.

- Clinical features of patients infected with 2019 novel coronavirus in Wuhan, China

- Imbalanced Host Response to SARS-CoV-2 Drives Development of COVID-19.

- SARS-CoV-2 Cell Entry Depends on ACE2 and TMPRSS2 and Is Blocked by a Clinically Proven Protease Inhibitor

- Type 1 interferons as a potential treatment against COVID-19.

Share this paper: 👍 🐦 in ✉

View more about this paper here: https://typeset.io/papers/type-i-interferon-susceptibility-distinguishes-sars-cov-2-
1fajselu8c

Type I interferon susceptibility distinguishes SARS-CoV-2 from SARS-CoV.

Kumari G. Lokugamage[1*], Adam Hage[1*], Maren de Vries[3], Ana M. Valero-Jimenez[3], Craig Schindewolf[1], Meike Dittmann[3], Ricardo Rajsbaum[1,2], Vineet D. Menachery[1,2]

[1]Department of Microbiology and Immunology, [2]Institute for Human Infection and Immunity, University of Texas Medical Branch, Galveston TX, USA

[3]Department of Microbiology, New York University School of Medicine, New York, NY 10016, USA

*Equal contributions

Corresponding Author: Vineet D. Menachery

Address: University of Texas Medical Branch, 301 University Blvd, Route #0610 Galveston, TX 77555

Email: Vimenach@utmb.edu

Article Summary: SARS-CoV-2 has similar replication kinetics to SARS-CoV, but demonstrates significant sensitivity to type I interferon treatment.

Running title: SARS-CoV-2 sensitive to type I IFN pretreatment

Keywords: Coronavirus, 2019-nCoV, SARS-CoV-2, COVID-19, SARS-CoV, type I interferon, IFN

1   **Abstract**

2   SARS-CoV-2, a novel coronavirus (CoV) that causes COVID-19, has recently emerged causing

3   an ongoing outbreak of viral pneumonia around the world. While distinct from SARS-CoV, both

4   group 2B CoVs share similar genome organization, origins to bat CoVs, and an arsenal of

5   immune antagonists. In this report, we evaluate type-I interferon (IFN-I) sensitivity of SARS-

6   CoV-2 relative to the original SARS-CoV. Our results indicate that while SARS-CoV-2

7   maintains similar viral replication to SARS-CoV, the novel CoV is much more sensitive to IFN-I.

8   In Vero and in Calu3 cells, SARS-CoV-2 is substantially attenuated in the context of IFN-I

9   pretreatment, while SARS-CoV is not. In line with these findings, SARS-CoV-2 fails to

10   counteract phosphorylation of STAT1 and expression of ISG proteins, while SARS-CoV is able

11   to suppress both. Comparing SARS-CoV-2 and influenza A virus in human airway epithelial

12   cultures (HAEC), we observe the absence of IFN-I stimulation by SARS-CoV-2 alone, but detect

13   failure to counteract STAT1 phosphorylation upon IFN-I pretreatment resulting in near ablation

14   of SARS-CoV-2 infection. Next, we evaluated IFN-I treatment post infection and found SARS-

15   CoV-2 was sensitive even after establishing infection. Finally, we examined homology between

16   SARS-CoV and SARS-CoV-2 in viral proteins shown to be interferon antagonists. The absence

17   of an equivalent open reading frame (ORF) 3b and changes to ORF6 suggest the two key IFN-I

18   antagonists may not maintain equivalent function in SARS-CoV-2. Together, the results identify

19   key differences in susceptibility to IFN-I responses between SARS-CoV and SARS-CoV-2 that

20   may help inform disease progression, treatment options, and animal model development.

21   **Importance**

22   With the ongoing outbreak of COVID-19, differences between SARS-CoV-2 and the original

23   SARS-CoV could be leveraged to inform disease progression and eventual treatment options.

24   In addition, these findings could have key implications for animal model development as well as

25   further research into how SARS-CoV-2 modulates the type I IFN response early during

26   infection.

Introduction

27

28   At the end of 2019, a cluster of patients in Hubei Province, China was diagnosed with a

29 viral pneumonia of unknown origins. With community links to the Huanan seafood market in

30 Wuhan, the disease cluster had echoes of the severe acute respiratory syndrome coronavirus

31 (SARS-CoV) outbreak that emerged at the beginning of the century (1). The 2019 etiologic

32 agent was identified as a novel coronavirus, 2019-nCoV, and subsequently renamed SARS-

33 CoV-2 (2). The new virus has nearly 80% nucleotide identity to the original SARS-CoV and the

34 corresponding CoV disease, COVID-19, has many of the hallmarks of SARS-CoV disease

35 including fever, breathing difficulty, bilateral lung infiltration, and death in the most extreme

36 cases (3, 4). In addition, the most severe SARS-CoV-2 disease corresponded to old age (>50

37 years old), health status, and healthcare workers, similar to both SARS- and MERS-CoV (5).

38 Together, the results indicate SARS-CoV-2 infection and disease have strong similarity to the

39 original SARS-CoV epidemic occurring nearly two decades earlier.

40   In the wake of the outbreak, major research efforts have sought to rapidly characterize

41 the novel CoV to aid in treatment and control. Initial modeling studies predicted (6) and

42 subsequent cell culture studies confirmed that spike protein of SARS-CoV-2 utilizes human

43 angiotensin converting enzyme 2 (ACE2) for entry, the same receptor as SARS-CoV (7, 8).

44 Extensive case studies indicated a similar range of disease onset and severe symptoms seen

45 with SARS-CoV (5). Notably, less severe SARS-CoV-2 cases have also been observed and

46 were not captured in the original SARS-CoV outbreak. Importantly, screening and treatment

47 guidance has relied on previous CoV data generated with SARS-CoV and MERS-CoV.

48 Treatments with both protease inhibitors and type-I interferon (IFN-I) have been employed (4);

49 similarly, remdesivir, a drug targeting viral polymerases, has been reported to have efficacy

50 against SARS-CoV-2 similar to findings with both SARS- and MERS-CoV (9-12). Importantly,

51 several vaccine efforts have been initiated with a focus on the SARS-CoV-2 spike protein as the

52 major antigenic determinant (13). Together, the similarities with SARS-CoV have been useful in

53 responding to the newest CoV outbreak.

54   The host innate immune response is initiated when viral products are recognized by host

55 cell pattern recognition receptors, including Toll-like receptors (TLRs) and RIG-I-like receptors

56 (RLRs) (14, 15). This response ultimately results in production of IFN-I and other cytokines,

57 which together are essential for an effective antiviral response (16). IFN-I then triggers its own

58 signaling cascade via its receptor, in an autocrine or paracrine manner, which induces

59 phosphorylation of signal transducers and activators of transcription 1 (STAT1) and STAT2.

60 Together, STAT1, STAT2, and a third transcription factor, IRF9, form the Interferon Stimulated

61 Gene Factor 3 (ISGF3) complex, which is essential for induction of many IFN-stimulated genes

62 (ISGs), and ultimately elicit an effective antiviral response (17, 18). To establish productive

63 replication, viruses have developed different mechanisms to escape this antiviral response

64 targeting different parts of the IFN-I response machinery (19).

65   In this study, we further characterize SARS-CoV-2 and compare it to the original SARS-

66 CoV. Using Vero E6 cells, we demonstrate that SARS-CoV-2 maintains similar viral replication

67 kinetics as SARS-CoV following a low dose infection. In contrast, we find that SARS-CoV-2 is

68 significantly more sensitive to IFN-I pretreatment as compared to SARS-CoV. Infection of IFN-I

69 competent Calu3 2B4 cells resulted in reduced SARS-CoV-2 replication compared to SARS-

70 CoV. Similar to Vero cells, Calu3 cells pretreated with IFN-I had a greater reduction of

71 replication of SARS-CoV-2 compared to SARS-CoV. In human airway epithelial cultures, SARS-

72 CoV-2 showed robust replication and an absence of IFN-I stimulation contrasting influenza A

73 virus. However, pretreatment with IFN-I confirmed SARS-CoV-2 sensitivity and inability to

74 control IFN-I responses once initiated. These results suggest distinct changes between SARS-

75 CoV and SARS-CoV-2 in terms of IFN-I antagonism and we subsequently examined sequence

76 homology between the SARS-CoV and SARS-CoV-2 viral proteins that may be responsible for

77 these differences. Together, the results suggest SARS-CoV-2 lacks the same capacity to

78 control the IFN-I response as SARS-CoV.

79 **Results**

80 **SARS-CoV-2 is sensitive to IFN-I pre-treatment**

81   Our initial studies infected Vero E6 cells using a low multiplicity of infection (MOI) to

82 explore the viral replication kinetics of SARS-CoV-2 relative to SARS-CoV. Following infection,

83 we found that both SARS-CoV and SARS-CoV-2 replicate with similar kinetics, peaking 48

84 hours post infection (**Fig. 1A**). While SARS-CoV-2 titer was slightly lower than that of SARS-

85 CoV at 24 hours post infection, the results were not statistically different. By 48 hours,

86 replication of both viruses had plateaued and significant cytopathic effect (CPE) was observed

87 for both SARS-CoV and SARS-CoV-2 infections. Together, the results indicated that SARS-CoV

88 and SARS-CoV-2 replicate with similar replication kinetics in Vero E6 cells.

89   We next evaluated the susceptibility of SARS-CoV-2 to IFN-I pretreatment. Treatment

90 with IFN-I (recombinant IFN-α) has been attempted as an antiviral approach for a wide variety of

91 pathogens including hepatitis B and C viruses as well as HIV (20). During both the SARS and

92 MERS-CoV outbreaks, IFN-I has been employed with limited effect (21, 22). In this study, we

93 pretreated Vero E6 cells with 1000 U/mL of recombinant IFN-I (IFN-α) 18 hours prior to

94 infection. Vero E6 lack the capacity to produce IFN-I, but are able to respond to exogenous

95 treatment (23). Following pretreatment with IFN-I, SARS-CoV infection has a modest reduction

96 in viral titer of 1.5 $\log_{10}$ plaque forming units (PFU) as compared to untreated control 24 hours

97 post infection (**Fig. 1A**). However, by 48 hours, SARS-CoV has nearly equivalent viral yields as

98 the untreated conditions (7.2 $\log_{10}$PFU versus 7.5 $\log_{10}$PFU). In contrast, SARS-CoV-2 shows a

99 significant reduction in viral replication following IFN-I treatment. At both 24 and 48 hours post

100 infection, SARS-CoV-2 had massive 3-$\log_{10}$ (24 HPI) and 4-$\log_{10}$ (48 HPI) drops in viral titer as

101   compared to control untreated cells. Together, the results demonstrate a clear sensitivity to a

102   primed IFN-I response in SARS-CoV-2, which is not observed with SARS-CoV.

103   To explore differences in IFN-I antagonism between SARS-CoV and SARS-CoV-2, we

104   examined both STAT1 activation and IFN stimulated gene (ISG) expression following IFN-I

105   pretreatment and infection. Examining Vero cell protein lysates, we found that IFN-I treated cells

106   infected with SARS-CoV-2 induced phosphorylated STAT1 by 48 hours post infection (**Fig. 1B**).

107   SARS-CoV had no evidence of STAT1 phosphorylation in either IFN-I treated or untreated cells,

108   illustrating robust control over IFN-I signaling pathways. In contrast, SARS-CoV-2 is unable to

109   control signaling upon IFN-I treatment. Examining further, IFITM1, a known ISG (17), had

110   increased protein expression in the context of SARS-CoV-2 infection following IFN-I

111   pretreatment compared to SARS-CoV under the same conditions (**Fig. 1B**). Basal STAT1 levels

112   are reduced during SARS-CoV infection relative to uninfected control and to a lesser extent

113   during SARS-CoV-2, likely due to the mRNA targeting activity of non-structural protein 1 (NSP1)

114   (24). However, IFN-I treatment results in augmented protein levels for IFITM1 following SARS-

115   CoV-2 infection as compared to untreated SARS-CoV-2. In contrast, IFN-I treated SARS-CoV

116   had no significant increase in IFITM1 relative to control infection. Together, the STAT1

117   phosphorylation, ISG production, and viral protein levels indicate that SARS-CoV-2 lacks the

118   same capacity to modulate the IFN-I stimulated response as the original SARS-CoV.

119   **SARS-CoV-2 attenuated in interferon competent cells.**

120   While capable of responding to exogenous IFN-I, Vero cells lack the capacity to produce

121   IFN-I following infection which likely plays a role in supporting robust replication of a wide range

122   of viruses. To evaluate SARS-CoV-2 in a IFN-I responsive cell type, we infected Calu3 2B4

123   cells, a lung epithelial cell line sorted for ACE2 expression and previously used in coronavirus

124   and influenza research (25). Using an MOI of 1, we examined the viral replication kinetics of

125   SARS-CoV-2 relative to SARS-CoV in Calu3 cells. We found that both SARS-CoV and SARS-

126   CoV-2 replicate with similar overall kinetics, peaking 24 hours post infection (**Fig. 2A**). However,

127   SARS-CoV-2 replication is slightly attenuated relative to SARS-CoV at 24 hours post infection

128   (0.82 $\log_{10}$ reduction).   The attenuation in viral replication expands at 48 hours (1.4 $\log_{10}$

129   reduction) indicating a significant change in total viral titers between SARS-CoV and SARS-

130   CoV-2. Notably, no similar attenuation was observed in untreated Vero cells (**Fig. 1A**)

131   suggesting possible immune modulation of SARS-CoV-2 infection in the respiratory cell line,

132   due to differential sensitivity to secreted IFN-I during infection. We next evaluated the

133   susceptibility of SARS-CoV-2 to IFN-I pretreatment in Calu3 cells. When pretreating cells with

134   1000 U/mL of recombinant IFN-I 18 hours prior to infection, SARS-CoV infection has a modest

135   reduction in viral titer of ~0.8 $\log_{10}$ PFU as compared to untreated control at both 24 and 48

136   hours post infection (**Fig. 2A**). Similar to Vero cell results, SARS-CoV-2 shows a significant

137   reduction in viral replication following IFN-I treatment in Calu3 cells. At both 24 and 48 hours

138   post infection, SARS-CoV-2 had 2.65- $\log_{10}$ (24 HPI) and 2- $\log_{10}$ (48 HPI) drops in viral titer,

139   respectively, as compared to control untreated Calu3 cells. Together, the results demonstrate a

140   clear sensitivity to a primed IFN-I response in SARS-CoV-2, which is not observed with SARS-

141   CoV.

142   To further evaluate activation by IFN-I, we examined both STAT1 phosphorylation and

143   ISG expression following infection of Calu3 2B4 cells at 48 hours. Probing cell protein lysates,

144   we found that untreated cells infected with SARS-CoV or SARS-CoV-2 induced phosphorylated

145   STAT1 by 48 hours post infection (**Fig. 2B**). However, the level of STAT1 is markedly

146   diminished in SARS-CoV infection as compared to SARS-CoV-2 suggesting the original

147   epidemic strain disrupts the expression of the ISG. The diminished STAT1 levels in SARS-CoV

148   correspond to robust spike expression in untreated cells. In contrast, SARS-CoV-2 spike is

149   reduced as compared to SARS-CoV, consistent with lower replication observed in untreated

150   Calu3 cells (**Fig. 2A**). The noticeable IFITM1 expression levels observed in untreated Calu3

151 cells infected with SARS-CoV-2 that were not observed in Vero cells may signify higher ISG

152 levels in Calu3 cells during SARS-CoV-2 infection and may contribute to its attenuation relative

153 to SARS-CoV.

154   Following IFN-I pretreatment in Calu3 cells the differences in STAT1 activation and ISG

155 induction are less prominent compared the Vero experiments, likely due to an already induced

156 IFN-I response to the virus infection. However, we still found a reduction in STAT1

157 phosphorylation and ISG induction in IFN-I pretreated SARS-CoV versus SARS-CoV-2

158 infection. Total STAT1 levels were augmented in IFN-I treated cells following SARS-CoV

159 infection to values similar to control IFN-I treated cells. In contrast, SARS-CoV-2 STAT1 levels

160 remained amplified relative to SARS-CoV, but were similar to untreated SARS-CoV-2 infection.

161 Although marginal, IFITM1 expression was slightly increased in IFN-I pretreatment SARS-CoV-

162 2 relative to SARS-CoV. Importantly, the spike protein levels show a significant impact of IFN-I

163 on SARS-CoV infection consistent with titer. For SARS-CoV-2, the spike blot demonstrates the

164 massive attenuation in the presence of IFN-I. Overall, the results in Calu3 cells are consistent

165 with Vero cell findings and indicate a significant sensitivity of SARS-CoV-2 to IFN-I

166 pretreatment.

167 **SARS-CoV-2 blocks IFN-I signaling in polarized human airway epithelial cultures.**

168 Having established IFN-I sensitivity in Vero cells and Calu3 respiratory cell lines, we next sought

169 to evaluate SARS-CoV-2 in polarized human airway epithelial cultures (HAEC). These cultures

170 provide both the complexity of different cell types and the architecture of the human respiratory

171 epithelium. Previous work with SARS-CoV had already established its capacity to control the

172 IFN-I response in human airway cultures (26). Therefore, to examine the impact on overall level

173 of IFN-I signaling in HAECs, we compared SARS-CoV-2 infection to influenza A virus (H1N1)

174 infection, known to induce robust innate immune responses in these cultures. Briefly, HAEC

175 were pretreated with IFN-α on the basolateral side prior to and during infection (**Fig. 3A**). Apical

176   washes were collected at multiple time points and analyzed for viral infectious titers by plaque

177   assay. In addition, culture lysates at endpoint were examined for STAT1 phosphorylation by

178   western blot. Both influenza A and SARS-CoV-2 triggered different levels of immune stimulation

179   (**Fig. 3B**).   Influenza A virus infection alone induced robust expression of both total and

180   phosphorylated STAT1 48 hours post infection. In stark contrast, SARS-CoV-2 infection alone

181   indicated no increase in STAT1 or phosphorylated STAT1. IFN-I pretreatment resulted in robust

182   induction of STAT1 and pSTAT1 in all cultures. Despite the distinct immune stimulation profiles

183   upon infection alone, both viruses robustly replicated in the HAEC, with influenza A virus

184   achieving higher viral yields as compared to SARS-CoV-2 (**Fig. 3C & 3D**). Pretreatment

185   reduced influenza infection ~1.5 $\log_{10}$ at both 24 and 48 hours post infection, consistent with

186   previous reports (27). In contrast, IFN-I pretreatment nearly ablated SARS-CoV-2 with 2-$\log_{10}$

187   and 4-$\log_{10}$ reduction in viral titers at 24 and 48 hours relative to untreated controls. Together,

188   the results highlight the capacity of SARS-CoV-2 to prevent IFN-I signaling, but also

189   demonstrate the sensitivity of SARS-CoV-2 to IFN-I pretreatment.

190   **SARS-CoV-2 impacted by IFN-I post treatment**. Having established that SARS-CoV-2 cannot

191   overcome a pre-induced IFN-I state, we next evaluated the impact of IFN-I treatment post

192   infection. Vero cells were infected with SARS-CoV or SARS-CoV-2 at an MOI 0.01 and

193   subsequently treated with 1000 U/mL IFN-α four hours post infection. For SARS-CoV, treatment

194   post infection had no significant impact on viral yields either 24 or 48 hours post infection,

195   consistent with findings from pretreatment experiments.   In contrast, SARS-CoV-2 had a

196   substantial 2-$\log_{10}$ reduction in viral titers at 24 hours post infection relative to control. However,

197   by 48 hours, SARS-CoV-2 replication had achieved similar level to untreated controls indicating

198   that post treatment had only a transient impact in Vero cells. We subsequently performed the

199   post-treatment experiment utilizing Calu3 respiratory cells at an MOI 1. Similar to Vero cells,

200   SARS-CoV infection post treatment resulted in no significant changes at 24 hours and has a

201 modest decrease (~0.5 $\log_{10}$) at 48 hours, illustrating its resistance to IFN-I. In contrast, IFN-I

202 post-treatment of SARS-CoV-2 infection resulted in a >2-$\log_{10}$ reduction in viral titers at 24 hours

203 and expanded at 48 hours post (~4-$\log_{10}$ reduction). The results indicate that in Calu3 cells,

204 SARS-CoV-2 is unable to prevent inhibitory effects of IFN-I even after establishing initial

205 infection. Overall, the pre- and post-treatment data highlight distinct differences between

206 SARS-CoV and SARS-CoV-2 in modulation of IFN-I pathways.

Conservation of IFN-I antagonists across SARS-CoV and SARS-CoV-2

208 Previous work has established several key IFN-I antagonists in the SARS-CoV genome,

209 including NSP1, NSP3, ORF3b, ORF6, and others (28). Considering SARS-CoV-2's sensitivity

210 to IFN-I, we next sought to evaluate conservation of IFN-I antagonist proteins encoded by

211 SARS-CoV-2, SARS-CoV, and several bat SARS-like viruses including WIV16-CoV (29),

212 SHC014-CoV (30), and HKU3.1-CoV (31). Using sequence analysis, we found several changes

213 to SARS-CoV-2 that potentially contribute to IFN-I sensitivity (**Fig. 4**). For SARS-CoV structural

214 proteins, including the nucleocapsid (N) and matrix (M) protein, a high degree of sequence

215 homology (>90%AA identity) suggests that their reported IFN-I antagonism is likely maintained

216 in SARS-CoV-2 and other SARS-like viruses. Similarly, the ORF1ab poly-protein retains high

217 sequence identity in SARS-CoV-2 and several known IFN-I antagonists contained within the

218 poly-protein (NSP1, NSP7, NSP14-16) are highly conserved relative to SARS-CoV. One notable

219 exception is the large papain-like protease, NSP3, which is only 76% conserved between

220 SARS-CoV and SARS-CoV-2. However, SARS-CoV-2 does maintain a deubiquitinating domain

221 thought to confer IFN-I resistance (32). For SARS-CoV ORF3b, a 154 amino acid (AA) protein

222 known to antagonize IFN-I responses by blocking IRF3 phosphorylation (33), sequence

223 alignment indicates that the SARS-CoV-2 equivalent ORF3b contains a premature stop codon

224 resulting in a truncated 24 AA protein. Similarly, HKU3.1-CoV also has a premature termination

225 resulting in a predicted 39 AA protein. Both WIV16-CoV and SHC014-CoV, the most closely

226   related bat viruses to SARS-CoV, encode longer 114 AA truncated protein with >99% homology

227   with SARS-CoV ORF3b suggesting that IFN-I antagonism might be maintained in these specific

228   group 2B CoV strains. In addition, SARS-CoV ORF6 has been shown to be an IFN-I antagonist

229   that disrupts karyopherin-mediated transportation of transcription factors like STAT1 (33, 34). In

230   contrast to ORF3b, all five surveyed group 2B CoVs maintain ORF6; however, SARS-CoV-2

231   had only 69% homology with SARS-CoV while the other three group 2B bat CoVs had >90%

232   conservation. Importantly, SARS-CoV-2 has a two amino acid truncation in its ORF6; previous

233   work has found that alanine substitution in this C-terminus of SARS-CoV ORF6 resulted in

234   ablated antagonism (34). Together, the sequence homology analysis suggests that differences

235   in NSP3, ORF3b, and/or ORF6 may be key drivers of SARS-CoV-2 IFN-I susceptibility.

236   **Discussion**

237   With the ongoing outbreak of COVID-19 caused by SARS-CoV-2, viral characterization remains

238   a key factor in responding to the emergent novel virus. In this report, we describe differences in

239   the IFN-I sensitivity between SARS-CoV-2 and the original SARS-CoV. While both viruses

240   maintain similar replication in untreated Vero E6 cells, SARS-CoV-2 has a significant decrease

241   in viral protein and replication following IFN-I pretreatment. The decreased SARS-CoV-2

242   replication correlates with phosphorylation of STAT1 and augmented ISG expression largely

243   absent following SARS-CoV infection despite IFN-I pretreatment. Infection of IFN-I competent

244   Calu3 2B4 cells resulted in reduced SARS-CoV-2 replication relative to SARS-CoV; IFN-I

245   pretreatment also corresponded to increased sensitivity for SARS-CoV-2 in Calu3 cells.

246   However, SARS-CoV-2 fails to induce IFN-I pathways during infection of unprimed polarized

247   HAEC as compared to influenza A virus, suggesting a capacity to control IFN-I signaling. Yet,

248   pretreatment nearly ablates replication of SARS-CoV-2 highlighting robust sensitivity to IFN-I

249   pathways once activated. Finally, SARS-CoV-2, unlike SARS-CoV, responded to post-infection

250   IFN-I treatment with reduced viral yields in both Vero and Calu3 cells. Analysis of viral proteins

251 finds SARS-CoV-2 has several changes that potentially impact its capacity to modulate the IFN-

252 I response, including loss of an equivalent ORF3b and a short truncation of ORF6, both known

253 as IFN-I antagonists for SARS-CoV (33). Together, our results suggest SARS-CoV and SARS-

254 CoV-2 have differences in their ability to antagonize the IFN-I response once initiated and that

255 this may have major implications for COVID-19 disease and treatment.

256   With a similar genome organization and disease symptoms in humans, the SARS-CoV-2

257 outbreak has drawn insights from the closely related SARS-CoV. However, the differences in

258 sensitivity to IFN-I pretreatment illustrate a clear distinction between the two CoVs. Coupled with

259 a novel furin cleavage site (35), robust upper airway infection (8), and transmission prior to

260 symptomatic disease (36), the differences between SARS-CoV and SARS-CoV-2 could prove

261 important in disrupting the ongoing spread of COVID-19. For SARS-CoV, *in vitro* studies have

262 consistently found that wild-type SARS-CoV is indifferent to IFN-I pretreatment (37, 38).

263 Similarly, *in vivo* SARS-CoV studies have found that the loss of IFN-I signaling had no

264 significant impact on disease (39), suggesting that this virus is not sensitive to the antiviral

265 effects of IFN-I. However, more recent reports suggest that host genetic background may

266 majorly influence this finding (40). For SARS-CoV-2, our results suggest that IFN-I pretreatment

267 produces a 3 - 4 $\log_{10}$ drop in viral titer. This level of sensitivity is similar to MERS-CoV and

268 suggests that the novel CoV lacks the same capacity to escape a primed IFN-I response as

269 SARS-CoV (41, 42). Notably, the sensitivity to IFN-I does not completely ablate viral replication;

270 unlike SARS-CoV 2'O methyl-transferase mutants (37), SARS-CoV-2 is able to replicate to low,

271 detectable levels even in the presence of IFN-I. This finding could help explain positive test

272 results in patients with minimal symptoms and the range of disease observed. In addition, while

273 SARS-CoV-2 is sensitive to IFN-I pretreatment, both SARS-CoV and MERS-CoV employ

274 effective means to disrupt virus recognition and downstream signaling until late during infection

275 (25). While SARS-CoV-2 may employ a similar mechanism early during infection, STAT1

276   phosphorylation and reduced viral replication are observed in IFN-I primed and post-treatment

277   conditions indicating that the novel CoV does not block IFN-I signaling as effectively as the

278   original SARS-CoV.

279   For SARS-CoV-2, the sensitivity to IFN-I indicates a distinction from SARS-CoV and

280   suggests differential host innate immune modulation between the viruses. The distinct ORF3b

281   and truncation/changes in ORF6 could signal a reduced capacity of SARS-CoV-2 to interfere

282   with IFN-I responses. For SARS-CoV ORF6, the N-terminal domain has been shown to have a

283   clear role in its ability to disrupt karyopherin-mediated STAT1 transport (34); in turn, the loss or

284   reduction of ORF6 function for SARS-CoV-2 would likely render it much more susceptible to

285   IFN-I pretreatment as activated STAT1 has the capacity to enter the nucleus and induce ISGs

286   and the antiviral response. In these studies, we have found that following IFN-I pretreatment,

287   STAT1 phosphorylation is induced following SARS-CoV-2 infection. The increase in ISG

288   proteins (STAT1, IFITM1) suggests that SARS-CoV-2 ORF6 does not effectively block nuclear

289   transport as well as SARS-CoV ORF6. For SARS-CoV ORF3b, the viral protein has been

290   shown to disrupt phosphorylation of IRF3, a key transcriptional factor in the production of IFN-I

291   and the antiviral state (33). While its mechanism of action is not clear, the ORF3b absence in

292   SARS-CoV-2 infection likely impacts its ability to inhibit the IFN-I response and eventual STAT1

293   activation. Similarly, while NSP3 deubiquitinating domain remains intact, SARS-CoV-2 has a 24

294   AA insertion upstream of this deubiquitinating domain that could potentially alter that function

295   (32). While other antagonists are maintained with high levels of conservation (>90%), single

296   point mutations in key locations could modify function and contribute to increased IFN-I

297   sensitivity. Overall, the sequence analysis suggests that differences between SARS-CoV and

298   SARS-CoV-2 viral proteins may drive attenuation in the context of IFN-I pretreatment.

299   The increased sensitivity of SARS-CoV-2 suggests utility in treatment using IFN-I. While

300   IFN-I has been used in response to chronic viral infection (43), previous examination of SARS-

301 CoV cases found inconclusive effect for IFN-I treatment (44). However, the findings from the

302 SARS-CoV outbreak were complicated by combination therapy of IFN-I with other treatments

303 including ribavirin/steroids and lack of a regimented protocol. While IFN-I has been utilized to

304 treat MERS-CoV infected patients, no conclusive data yet exists to determine efficacy (45). Yet,

305 *in vivo* studies with MERS-CoV have found that early induction with IFN-I can be protective in

306 mice (46); importantly, the same study found that late IFN-I activation can be detrimental for

307 MERS-CoV disease (46). Similarly, early reports have described treatments using IFN-I in

308 combination for SARS-CoV-2 infection; yet the efficacy of these treatments and the parameters

309 of their use are not known (47). Overall, sensitivity data suggest that IFN-I treatment may have

310 utility for treating SARS-CoV-2 if the appropriate parameters can be determined. In addition, use

311 of type III IFN, which is predicted to have utility in the respiratory tract, could offer another

312 means for effective treatment for SARS-CoV-2.

313 In addition to treatment, the sensitivity to IFN-I may also have implications for animal

314 model development. For SARS-CoV, mouse models that recapitulate human disease were

315 developed through virus passage in immune competent mice (48). Similarly, mouse models for

316 MERS-CoV required adaptation in mice that had genetic modifications of their dipeptidyl-

317 peptidase 4 (DPP4), the receptor for MERS-CoV (49, 50). However, each of these MERS-CoV

318 mouse models still retained full immune capacity. In contrast, SARS-CoV-2 sensitivity to IFN-I

319 may signal the need to use an immune deficient model to develop relevant disease. While initial

320 work has suggested incompatibility to SARS-CoV-2 infection in mice based on receptor usage

321 (8), the IFN-I response may be a second major barrier that needs to be overcome. Similar to

322 the emergent Zika virus outbreak, the use of IFN-I receptor knockout mice or IFN-I receptor

323 blocking antibody may be necessary to develop a useful SARS-CoV-2 animal models for

324 therapeutic testing (51).

325   Overall, our results indicate that SARS-CoV-2 has a much higher sensitivity to type I IFN

326 than the previously emergent SARS-CoV. This augmented type I IFN sensitivity is likely due to

327 changes in viral proteins between the two epidemic CoV strains. Moving forward, these data

328 could provide important insights for both the treatment of SARS-CoV-2 as well as developing

329 novel animal models of disease. In this ongoing outbreak, the results also highlight a distinction

330 between the highly related viruses and suggest insights from SARS-CoV must be verified for

331 SARS-CoV-2 infection and disease.

332

Methods

Viruses and cells. SARS-CoV-2 USA-WA1/2020 was provided by the World Reference Center for Emerging Viruses and Arboviruses (WRCEVA) or BEI Resources and was originally obtained from the USA Centers of Disease Control as described (52). SARS-CoV-2 and mouse-adapted recombinant SARS-CoV (MA15) (48) were titrated and propagated on Vero E6 cells, grown in DMEM with 5% fetal bovine serum and 1% antibiotic/antimytotic (Gibco). Calu3 2B4 cells were grown in DMEM with 10% defined fetal bovine serum, 1% sodium pyruvate (Gibco), and 1% antibiotic/antimitotic (Gibco). Standard plaque assays were used for SARS-CoV and SARS-CoV-2 (26, 53). All experiments involving infectious virus were conducted at the University of Texas Medical Branch (Galveston, TX) or New York University School of Medicine (New York City, NY) in approved biosafety level 3 (BSL) laboratories with routine medical monitoring of staff.

Infection and type I IFN pre- and post-treatment. Viral replication studes in Vero E6 and Calu3 2B4 cells were performed as previously described (37, 54). Briefly, cells were washed two times with PBS and inoculated with SARS-CoV or SARS-CoV-2 at a multiplicity of infection (MOI) 0.01 for 60 minutes at 37 °C. Following inoculation, cells were washed 3 times, and fresh media was added to signify time 0. Three or more biological replicates were harvested at each described time. No blinding was used in any sample collections, nor were samples randomized. For type I IFN pretreatment, experiments were completed as previously described (37). Briefly, Vero E6 cells were incubated with 1000 U/mL of recombinant type I IFN-α (PBL Assay Sciences) 18 hours prior to infection (37). Cells were infected as described above and type I IFN was not added back after infection.

Generation of polarized human airway epithelial cultures (HAEC).

356   hTert-immortalized human normal airway tracheobronchial epithelial cells, BCi.NS1.1 (55) were

357   maintained in ExPlus growth media (StemCell). To generate HAEC, BCi.NS1.1 were plated

358   (7.5E4 cells/well) on rat-tail collagen type 1-coated permeable transwell membrane supports

359   (6.5mm; Corning Inc), immersed in ExPlus growth media in both the apical and basal chamber.

360   Upon reaching confluency, media in the apical chamber was removed (airlift), and media in the

361   basal chamber was changed to Pneumacult ALI maintenance media (StemCell). Pneumacult

362   ALI maintenance media was changed every two days for approximately 6 weeks to form

363   differentiated, polarized cultures that resemble in vivo pseudostratified mucociliary epithelium.

364   **IFN-I treatment and infection of HAEC.**

365   For interferon pretreatment of human airway epithelial cultures, 1000 U/mL of universal

366   recombinant interferon-alpha was added to the basolateral chamber 2 h prior to viral infections.

367   For viral infections, cultures were washed apically with 50 µl of prewarmed PBS three times for

368   30 min at 37°C. Virus inoculates (1.3E6 PFU for influenza A/California/07/2009 (H1N1) virus

369   and 1.35E5 PFU for SARS-CoV-2 USA/WA/1/2020 in 50 µl PBS Mg/Ca) were added apically for

370   two hours. Inoculates were then removed and cultures were washed three times with PBS, the

371   third wash was collected and then the cultures were incubated for the indicated times. Progeny

372   virus was collected in apical washes with 50 µl PBS Mg/Ca for 30 min at 8, 24 and 48 hpi

373   (endpoint). At endpoint, the membranes were collected and lysed in 300 µl LDS lysis buffer (Life

374   Technologies). Protein levels were measured by western blot. Briefly, 5 µl of cell lysates were

375   loaded into a SDS-PAGE gel and transferred to a nitrocellulose membrane. The membranes

376   were blocked for 1 h at room temperature with 5% skim milk and then incubated overnight at

377   4°C with appropriate primary antibody dilution: anti-STAT1 (1:1000, Cell Signaling), anti-

378   pSTAT1 (1:1000, Cell Signaling) or anti-beta actin (1:5000, Invitrogen). Then, the membranes

379   were incubated with the recommended dilution of HRP-conjugated secondary antibody (goat

380   anti-rabbit IgG HRP 1:10000, Invitrogen; goat anti-mouse IgG HRP 1:10000, Invitrogen) at room

381 temperature for 1 h. Super Signal West Dura Kit (Thermo Scientific) was used for signal

382 development according to manufacturer's recommendations and the chemiluminescence was

383 detected with a ChemiDoc Imager (BioRad).

384 **Phylogenetic Tree and Sequence Identity Heat Map**. Heat maps were constructed from a set

385 of representative group 2B coronaviruses by using alignment data paired with neighbor-joining

386 phylogenetic trees built in Geneious (v.9.1.5). Sequence identity was visualized using EvolView

387 (http://evolgenius.info/) and utilized SARS-CoV Urbani as the reference sequence. Tree shows

388 the degree of genetic similarity of SARS-CoV-2 and SARS-CoV across selected group 2B

389 coronaviruses.

390 **Immunoblot Analysis and Antibodies:**

391 Viral and host protein analysis were evaluated as previously described (52, 56). Briefly, cell

392 lysates were resolved on 7.5% Mini-PROTEAN TGX SDS-PAGE gels and then transferred to

393 polyvinylidene difluoride (PVDF) membranes using a Trans-Blot Turbo transfer system (Bio-

394 Rad). Membranes were blocked with 5% (w/v) non-fat dry milk in TBST (TBS with 0.1% (v/v)

395 Tween-20) for 1 hr, and then probed with the indicated primary antibody in 3% (w/v) BSA in

396 TBST at 4°C overnight. Following overnight incubation, membranes were probed with the

397 following secondary antibodies in 5% (w/v) non-fat dry milk in TBST for 1 hr at room

398 temperature: anti-rabbit or anti-mouse IgG-HRP conjugated antibody from sheep (both 1:10,000

399 GE Healthcare). Proteins were visualized using ECL or SuperSignal West Femto

400 chemiluminescence reagents (Pierce) and detected by autoradiography. The following primary

401 antibodies were used: anti-pSTAT1 (Y701) (1:1000 9171L Cell Signaling Technologies), anti-

402 STAT1 D1K9Y (1:1000 14994P Cell Signaling Technologies), anti-IFITM1 (1:1000 PA5-20989

403 Invitrogen), anti-SARS-CoV/CoV-2 Spike 1A9 (1:1000 GTX632604 GeneTex), and anti-β-Actin

404 (1:1000 ab8227 Abcam).

405   **Statistical analysis.** All statistical comparisons in this manuscript involved the comparison

406   between 2 groups, SARS-CoV or SARS-CoV-2 infected groups under equivalent conditions.

407   Thus, significant differences in viral titer were determined by the unpaired two-tailed student's T-

408   Test.

415

References

1. **Gralinski LE, Menachery VD.** 2020. Return of the Coronavirus: 2019-nCoV. Viruses **12**.

2. **Gorbalenya AE, Baker SC, Baric RS, de Groot RJ, Drosten C, Gulyaeva AA, Haagmans BL, Lauber C, Leontovich AM, Neuman BW, Penzar D, Perlman S, Poon LLM, Samborskiy DV, Sidorov IA, Sola I, Ziebuhr J, Coronaviridae Study Group of the International Committee on Taxonomy of V.** 2020. The species Severe acute respiratory syndrome-related coronavirus: classifying 2019-nCoV and naming it SARS-CoV-2. Nature Microbiology doi:10.1038/s41564-020-0695-z.

3. **Zhu N, Zhang D, Wang W, Li X, Yang B, Song J, Zhao X, Huang B, Shi W, Lu R, Niu P, Zhan F, Ma X, Wang D, Xu W, Wu G, Gao GF, Tan W, China Novel Coronavirus I, Research T.** 2020. A Novel Coronavirus from Patients with Pneumonia in China, 2019. N Engl J Med **382:**727-733.

4. **Huang C, Wang Y, Li X, Ren L, Zhao J, Hu Y, Zhang L, Fan G, Xu J, Gu X, Cheng Z, Yu T, Xia J, Wei Y, Wu W, Xie X, Yin W, Li H, Liu M, Xiao Y, Gao H, Guo L, Xie J, Wang G, Jiang R, Gao Z, Jin Q, Wang J, Cao B.** 2020. Clinical features of patients infected with 2019 novel coronavirus in Wuhan, China. Lancet **395:**497-506.

5. **Wu Z, McGoogan JM.** 2020. Characteristics of and Important Lessons From the Coronavirus Disease 2019 (COVID-19) Outbreak in China: Summary of a Report of 72314 Cases From the Chinese Center for Disease Control and Prevention. JAMA doi:10.1001/jama.2020.2648.

6. **Xu X, Chen P, Wang J, Feng J, Zhou H, Li X, Zhong W, Hao P.** 2020. Evolution of the novel coronavirus from the ongoing Wuhan outbreak and modeling of its spike protein for risk of human transmission. Sci China Life Sci **63:**457-460.

7. **Letko M, Marzi A, Munster V.** 2020. Functional assessment of cell entry and receptor usage for SARS-CoV-2 and other lineage B betacoronaviruses. Nat Microbiol doi:10.1038/s41564-020-0688-y.

8. **Zhou P, Yang XL, Wang XG, Hu B, Zhang L, Zhang W, Si HR, Zhu Y, Li B, Huang CL, Chen HD, Chen J, Luo Y, Guo H, Jiang RD, Liu MQ, Chen Y, Shen XR, Wang X, Zheng XS, Zhao K, Chen QJ, Deng F, Liu LL, Yan B, Zhan FX, Wang YY, Xiao GF, Shi ZL.** 2020. A pneumonia outbreak associated with a new coronavirus of probable bat origin. Nature doi:10.1038/s41586-020-2012-7.

9. **de Wit E, Feldmann F, Cronin J, Jordan R, Okumura A, Thomas T, Scott D, Cihlar T, Feldmann H.** 2020. Prophylactic and therapeutic remdesivir (GS-5734) treatment in the rhesus macaque model of MERS-CoV infection. Proc Natl Acad Sci U S A doi:10.1073/pnas.1922083117.

10. **Wang M, Cao R, Zhang L, Yang X, Liu J, Xu M, Shi Z, Hu Z, Zhong W, Xiao G.** 2020. Remdesivir and chloroquine effectively inhibit the recently emerged novel coronavirus (2019-nCoV) in vitro. Cell Res doi:10.1038/s41422-020-0282-0.

11. **Sheahan TP, Sims AC, Leist SR, Schafer A, Won J, Brown AJ, Montgomery SA, Hogg A, Babusis D, Clarke MO, Spahn JE, Bauer L, Sellers S, Porter D, Feng JY, Cihlar T, Jordan R, Denison MR, Baric RS.** 2020. Comparative therapeutic efficacy of remdesivir and combination lopinavir, ritonavir, and interferon beta against MERS-CoV. Nat Commun **11:**222.

12. **Sheahan TP, Sims AC, Graham RL, Menachery VD, Gralinski LE, Case JB, Leist SR, Pyrc K, Feng JY, Trantcheva I, Bannister R, Park Y, Babusis D, Clarke MO, Mackman RL, Spahn JE, Palmiotti CA, Siegel D, Ray AS, Cihlar T, Jordan R, Denison MR, Baric RS.** 2017. Broad-spectrum antiviral GS-5734 inhibits both epidemic and zoonotic coronaviruses. Sci Transl Med **9**.

13. **Ahmed SF, Quadeer AA, McKay MR.** 2020. Preliminary Identification of Potential Vaccine Targets for the COVID-19 Coronavirus (SARS-CoV-2) Based on SARS-CoV Immunological Studies. Viruses **12**.

466   14.   **Medzhitov R, Janeway CA, Jr.** 1997. Innate immunity: the virtues of a nonclonal
467   system of recognition. Cell **91:**295-298.
468   15.   **Meylan E, Tschopp J.** 2006. Toll-like receptors and RNA helicases: two parallel ways to
469   trigger antiviral responses. Mol Cell **22:**561-569.
470   16.   **Akira S.** 2006. TLR signaling. Curr Top Microbiol Immunol **311:**1-16.
471   17.   **Schoggins JW, Wilson SJ, Panis M, Murphy MY, Jones CT, Bieniasz P, Rice CM.**
472   2011. A diverse range of gene products are effectors of the type I interferon antiviral response.
473   Nature **472:**481-485.
474   18.   **Platanias LC.** 2005. Mechanisms of type-I- and type-II-interferon-mediated signalling.
475   Nat Rev Immunol **5:**375-386.
476   19.   **Rajsbaum R, Garcia-Sastre A.** 2013. Viral evasion mechanisms of early antiviral
477   responses involving regulation of ubiquitin pathways. Trends Microbiol **21:**421-429.
478   20.   **Lin FC, Young HA.** 2014. Interferons: Success in anti-viral immunotherapy. Cytokine
479   Growth Factor Rev **25:**369-376.
480   21.   **Zumla A, Hui DS, Perlman S.** 2015. Middle East respiratory syndrome. Lancet
481   **386:**995-1007.
482   22.   **Song Z, Xu Y, Bao L, Zhang L, Yu P, Qu Y, Zhu H, Zhao W, Han Y, Qin C.** 2019.
483   From SARS to MERS, Thrusting Coronaviruses into the Spotlight. Viruses **11**.
484   23.   **Diaz MO, Ziemin S, Le Beau MM, Pitha P, Smith SD, Chilcote RR, Rowley JD.** 1988.
485   Homozygous deletion of the alpha- and beta 1-interferon genes in human leukemia and derived
486   cell lines. Proc Natl Acad Sci U S A **85:**5259-5263.
487   24.   **Narayanan K, Ramirez SI, Lokugamage KG, Makino S.** 2015. Coronavirus
488   nonstructural protein 1: Common and distinct functions in the regulation of host and viral gene
489   expression. Virus Res **202:**89-100.
490   25.   **Menachery VD, Eisfeld AJ, Schafer A, Josset L, Sims AC, Proll S, Fan S, Li C,**
491   **Neumann G, Tilton SC, Chang J, Gralinski LE, Long C, Green R, Williams CM, Weiss J,**
492   **Matzke MM, Webb-Robertson BJ, Schepmoes AA, Shukla AK, Metz TO, Smith RD, Waters**
493   **KM, Katze MG, Kawaoka Y, Baric RS.** 2014. Pathogenic influenza viruses and coronaviruses
494   utilize similar and contrasting approaches to control interferon-stimulated gene responses. MBio
495   **5:**e01174-01114.
496   26.   **Sims AC, Tilton SC, Menachery VD, Gralinski LE, Schäfer A, Matzke MM, Webb-**
497   **Robertson BJ, Chang J, Luna ML, Long CE, Shukla AK, Bankhead AR, Burkett SE,**
498   **Zornetzer G, Tseng CT, Metz TO, Pickles R, McWeeney S, Smith RD, Katze MG, Waters**
499   **KM, Baric RS.** 2013. Release of severe acute respiratory syndrome coronavirus nuclear import
500   block enhances host transcription in human lung cells. J Virol **87:**3885-3902.
501   27.   **Österlund P, Pirhonen J, Ikonen N, Rönkkö E, Strengell M, Mäkelä SM, Broman M,**
502   **Hamming OJ, Hartmann R, Ziegler T, Julkunen I.** 2010. Pandemic H1N1 2009 Influenza A
503   Virus Induces Weak Cytokine Responses in Human Macrophages and Dendritic Cells and Is
504   Highly Sensitive to the Antiviral Actions of Interferons. Journal of Virology **84:**1414-1422.
505   28.   **Totura AL, Baric RS.** 2012. SARS coronavirus pathogenesis: host innate immune
506   responses and viral antagonism of interferon. Curr Opin Virol **2:**264-275.
507   29.   **Yang XL, Hu B, Wang B, Wang MN, Zhang Q, Zhang W, Wu LJ, Ge XY, Zhang YZ,**
508   **Daszak P, Wang LF, Shi ZL.** 2015. Isolation and Characterization of a Novel Bat Coronavirus
509   Closely Related to the Direct Progenitor of Severe Acute Respiratory Syndrome Coronavirus. J
510   Virol **90:**3253-3256.
511   30.   **Ge XY, Li JL, Yang XL, Chmura AA, Zhu G, Epstein JH, Mazet JK, Hu B, Zhang W,**
512   **Peng C, Zhang YJ, Luo CM, Tan B, Wang N, Zhu Y, Crameri G, Zhang SY, Wang LF,**
513   **Daszak P, Shi ZL.** 2013. Isolation and characterization of a bat SARS-like coronavirus that
514   uses the ACE2 receptor. Nature **503:**535-538.

515 31. **Lau SK, Woo PC, Li KS, Huang Y, Tsoi HW, Wong BH, Wong SS, Leung SY, Chan**
516 **KH, Yuen KY.** 2005. Severe acute respiratory syndrome coronavirus-like virus in Chinese
517 horseshoe bats. Proc Natl Acad Sci U S A **102:**14040-14045.
518 32. **Clementz MA, Chen Z, Banach BS, Wang Y, Sun L, Ratia K, Baez-Santos YM, Wang**
519 **J, Takayama J, Ghosh AK, Li K, Mesecar AD, Baker SC.** 2010. Deubiquitinating and
520 interferon antagonism activities of coronavirus papain-like proteases. J Virol **84:**4619-4629.
521 33. **Kopecky-Bromberg SA, Martinez-Sobrido L, Frieman M, Baric RA, Palese P.** 2007.
522 Severe acute respiratory syndrome coronavirus open reading frame (ORF) 3b, ORF 6, and
523 nucleocapsid proteins function as interferon antagonists. J Virol **81:**548-557.
524 34. **Frieman M, Yount B, Heise M, Kopecky-Bromberg SA, Palese P, Baric RS.** 2007.
525 Severe acute respiratory syndrome coronavirus ORF6 antagonizes STAT1 function by
526 sequestering nuclear import factors on the rough endoplasmic reticulum/Golgi membrane. J
527 Virol **81:**9812-9824.
528 35. **Coutard B, Valle C, de Lamballerie X, Canard B, Seidah NG, Decroly E.** 2020. The
529 spike glycoprotein of the new coronavirus 2019-nCoV contains a furin-like cleavage site absent
530 in CoV of the same clade. Antiviral Res **176:**104742.
531 36. **Tong ZD, Tang A, Li KF, Li P, Wang HL, Yi JP, Zhang YL, Yan JB.** 2020. Potential
532 Presymptomatic Transmission of SARS-CoV-2, Zhejiang Province, China, 2020. Emerg Infect
533 Dis **26**.
534 37. **Menachery VD, Yount BL, Jr., Josset L, Gralinski LE, Scobey T, Agnihothram S,**
535 **Katze MG, Baric RS.** 2014. Attenuation and restoration of severe acute respiratory syndrome
536 coronavirus mutant lacking 2'-o-methyltransferase activity. J Virol **88:**4251-4264.
537 38. **Thiel V, Weber F.** 2008. Interferon and cytokine responses to SARS-coronavirus
538 infection. Cytokine Growth Factor Rev **19:**121-132.
539 39. **Frieman MB, Chen J, Morrison TE, Whitmore A, Funkhouser W, Ward JM,**
540 **Lamirande EW, Roberts A, Heise M, Subbarao K, Baric RS.** 2010. SARS-CoV pathogenesis
541 is regulated by a STAT1 dependent but a type I, II and III interferon receptor independent
542 mechanism. PLoS Pathog **6:**e1000849.
543 40. **Channappanavar R, Fehr AR, Vijay R, Mack M, Zhao J, Meyerholz DK, Perlman S.**
544 2016. Dysregulated Type I Interferon and Inflammatory Monocyte-Macrophage Responses
545 Cause Lethal Pneumonia in SARS-CoV-Infected Mice. Cell Host Microbe **19:**181-193.
546 41. **Menachery VD, Gralinski LE, Mitchell HD, Dinnon KH, 3rd, Leist SR, Yount BL, Jr.,**
547 **Graham RL, McAnarney ET, Stratton KG, Cockrell AS, Debbink K, Sims AC, Waters KM,**
548 **Baric RS.** 2017. Middle East Respiratory Syndrome Coronavirus Nonstructural Protein 16 Is
549 Necessary for Interferon Resistance and Viral Pathogenesis. mSphere **2**.
550 42. **Falzarano D, de Wit E, Martellaro C, Callison J, Munster VJ, Feldmann H.** 2013.
551 Inhibition of novel beta coronavirus replication by a combination of interferon-alpha2b and
552 ribavirin. Sci Rep **3:**1686.
553 43. **Finter NB, Chapman S, Dowd P, Johnston JM, Manna V, Sarantis N, Sheron N,**
554 **Scott G, Phua S, Tatum PB.** 1991. The use of interferon-alpha in virus infections. Drugs
555 **42:**749-765.
556 44. **Stockman LJ, Bellamy R, Garner P.** 2006. SARS: systematic review of treatment
557 effects. PLoS Med **3:**e343.
558 45. **de Wit E, van Doremalen N, Falzarano D, Munster VJ.** 2016. SARS and MERS:
559 recent insights into emerging coronaviruses. Nat Rev Microbiol **14:**523-534.
560 46. **Channappanavar R, Fehr AR, Zheng J, Wohlford-Lenane C, Abrahante JE, Mack M,**
561 **Sompallae R, McCray PB, Jr., Meyerholz DK, Perlman S.** 2019. IFN-I response timing
562 relative to virus replication determines MERS coronavirus infection outcomes. J Clin Invest
563 **130:**3625-3639.
564 47. **Pang J, Wang MX, Ang IYH, Tan SHX, Lewis RF, Chen JI, Gutierrez RA, Gwee**
565 **SXW, Chua PEY, Yang Q, Ng XY, Yap RK, Tan HY, Teo YY, Tan CC, Cook AR, Yap JC, Hsu**

566 **LY.** 2020. Potential Rapid Diagnostics, Vaccine and Therapeutics for 2019 Novel Coronavirus
567 (2019-nCoV): A Systematic Review. J Clin Med **9**.
568 48.   **Roberts A, Deming D, Paddock CD, Cheng A, Yount B, Vogel L, Herman BD,**
569 **Sheahan T, Heise M, Genrich GL, Zaki SR, Baric R, Subbarao K.** 2007. A mouse-adapted
570 SARS-coronavirus causes disease and mortality in BALB/c mice. PLoS Pathog **3:**e5.
571 49.   **Cockrell A YB, Scobey T, Jensen K, Douglas M, Beall A, Tang X-C, Marasco WA,**
572 **Heise MT, Baric RS** 2016. A Mouse Model for MERS Coronavirus Induced Acute Respiratory
573 Distress Syndrome. . Nature Microbiology **In Press**.
574 50.   **Li K, Wohlford-Lenane CL, Channappanavar R, Park JE, Earnest JT, Bair TB, Bates**
575 **AM, Brogden KA, Flaherty HA, Gallagher T, Meyerholz DK, Perlman S, McCray PB, Jr.**
576 2017. Mouse-adapted MERS coronavirus causes lethal lung disease in human DPP4 knockin
577 mice. Proc Natl Acad Sci U S A **114:**E3119-E3128.
578 51.   **Lazear HM, Govero J, Smith AM, Platt DJ, Fernandez E, Miner JJ, Diamond MS.**
579 2016. A Mouse Model of Zika Virus Pathogenesis. Cell Host Microbe **19:**720-730.
580 52.   **Harcourt J, Tamin A, Lu X, Kamili S, Sakthivel SK, Murray J, Queen K, Tao Y,**
581 **Paden CR, Zhang J, Li Y, Uehara A, Wang H, Goldsmith C, Bullock HA, Wang L, Whitaker**
582 **B, Lynch B, Gautam R, Schindewolf C, Lokugamage KG, Scharton D, Plante JA,**
583 **Mirchandani D, Widen SG, Narayanan K, Makino S, Ksiazek TG, Plante KS, Weaver SC,**
584 **Lindstrom S, Tong S, Menachery VD, Thornburg NJ.** 2020. Severe Acute Respiratory
585 Syndrome Coronavirus 2 from Patient with 2019 Novel Coronavirus Disease, United States.
586 Emerg Infect Dis **26**.
587 53.   **Josset L, Menachery VD, Gralinski LE, Agnihothram S, Sova P, Carter VS, Yount**
588 **BL, Graham RL, Baric RS, Katze MG.** 2013. Cell host response to infection with novel human
589 coronavirus EMC predicts potential antivirals and important differences with SARS coronavirus.
590 MBio **4:**e00165-00113.
591 54.   **Sheahan T, Rockx B, Donaldson E, Corti D, Baric R.** 2008. Pathways of cross-
592 species transmission of synthetically reconstructed zoonotic severe acute respiratory syndrome
593 coronavirus. J Virol **82:**8721-8732.
594 55.   **Walters MS, Gomi K, Ashbridge B, Moore MA, Arbelaez V, Heldrich J, Ding BS,**
595 **Rafii S, Staudt MR, Crystal RG.** 2013. Generation of a human airway epithelium derived basal
596 cell line with multipotent differentiation capacity. Respir Res **14:**135.
597 56.   **van Tol S, Atkins C, Bharaj P, Johnson KN, Hage A, Freiberg AN, Rajsbaum R.**
598 2020. VAMP8 Contributes to the TRIM6-Mediated Type I Interferon Antiviral Response during
599 West Nile Virus Infection. J Virol **94**.

600

601

602 **Figure Legends**

603 **Figure 1. SARS-CoV-2 sensitive to type I IFN pretreatment.** A) Vero E6 cells were treated

604 with 1000 U/mL recombinant type I (hashed line) IFN or mock (solid line) for 18 hours prior to

605 infection. Cells were subsequently infected with either SARS-CoV WT (black) or SARS-CoV-2

606 (blue) at an MOI of 0.01 as described above. Each point on the line graph represents the group

607 mean, N ≥ 3. All error bars represent SD. The two tailed students t-test was used to determine

608 P-values: *** P < 0.001. B) Vero cell protein lysates from IFN-I treated and untreated cells were

609 probed 48 hours post infection by Western blotting for phosphorylated STAT1 (Y701), STAT1,

610 IFITM1, SARS spike, and Actin.

611 **Figure 2. SARS-CoV-2 attenuated and IFN-I sensitive in Calu3 respiratory cells.** A) Calu3

612 2B4 cells were treated with 1000 U/mL recombinant type I (hashed line) IFN or mock (solid line)

613 for 18 hours prior to infection. Cells were subsequently infected with either SARS-CoV WT

614 (black) or SARS-CoV-2 (blue) at an MOI of 1. Each point on the line graph represents the

615 group mean, N ≥ 3. All error bars represent SD. The two tailed students t-test was used to

616 determine P-values: *** P < 0.001. B) Calu3 cell protein lysates from IFN-I treated and untreated

617 cells were probed 48 hours post infection by Western blotting for phosphorylated STAT1 (Y701),
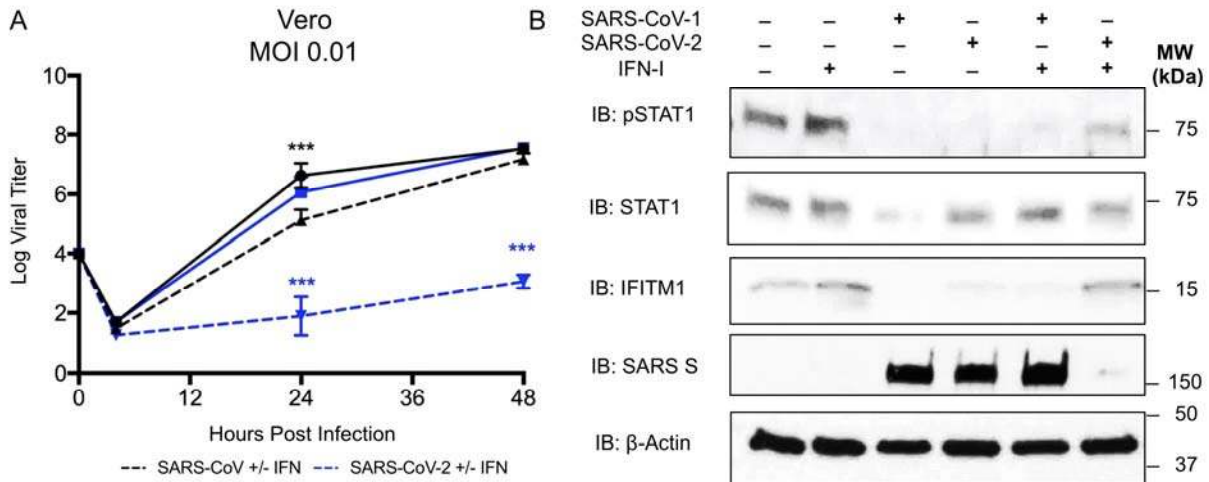
618 STAT1, IFITM1, SARS spike, and Actin.

619 **Figure 3. Differential IFN-I sensitivity and pSTAT1 phosphorylation following SARS-CoV-**

620 **2 or influenza A virus on polarized human airway epithelial cultures (HAEC**). A) HAEC

621 were pretreated with 1000 U/mL IFN-α basolaterally for 2 hours prior to and during infection.

622 Cultures were then infected apically with influenza A/California/09 H1N1 virus or SARS-CoV-2.

623 Apical washes were collected at the indicated times and progeny titers determined by plaque

624 assay on MDCK cells (influenza virus) or Vero E6 cells (SARS-CoV-2). At the 48 h endpoint,

625 cultures were lysed for western blot analysis. B) Western for total STAT1 or phospho-STAT1 at

626 48 hpi, and actin as loading control. C) Influenza A virus titers by plaque assay on MDCK cells.

627   0 h, virus inoculate; 2 h, virus in third apical wash; 8, 24, 48 h, virus in apical washes at these

628   time points. D) SARS-CoV-2 titers by plaque assay on Vero E6 cells. 0 h, virus inoculate; 2 h,

629   virus in second apical wash; 8, 24, 48 h, virus in apical washes at these time points.

630   **Figure 4, SARS-CoV-2 impacted by post IFN-I treatment.** A-B) Vero E6 and Calu3 2B4 cells

631   were infected with either SARS-CoV WT (black) or SARS-CoV-2 (blue) at an MOI 0.01 (A, Vero

632   cells) or MOI 1 (B, Calu3 cells). Cells were subsequently treated with 1000 U/mL recombinant

633   type I IFN (hashed line) or mock (solid line) for 4 hours following infection. Each point on the line

634   graph represents the group mean, N ≥ 3. All error bars represent SD. The two tailed student's t-

635   test was used to determine P-values: **P <0.01 *** P < 0.001.

636   **Figure 5, Conservation of SARS-CoV IFN antagonists.** Viral protein sequences of the

637   indicated viruses were aligned according to the bounds of the SARS-CoV open reading frames

638   for each viral protein. Sequence identities were extracted from the alignments for each viral

639   protein, and a heat map of percent sequence identity was constructed using EvolView

640   (www.evolgenius.info/evolview) with SARS-CoV as the reference sequence. TR = truncated

641   protein.

642
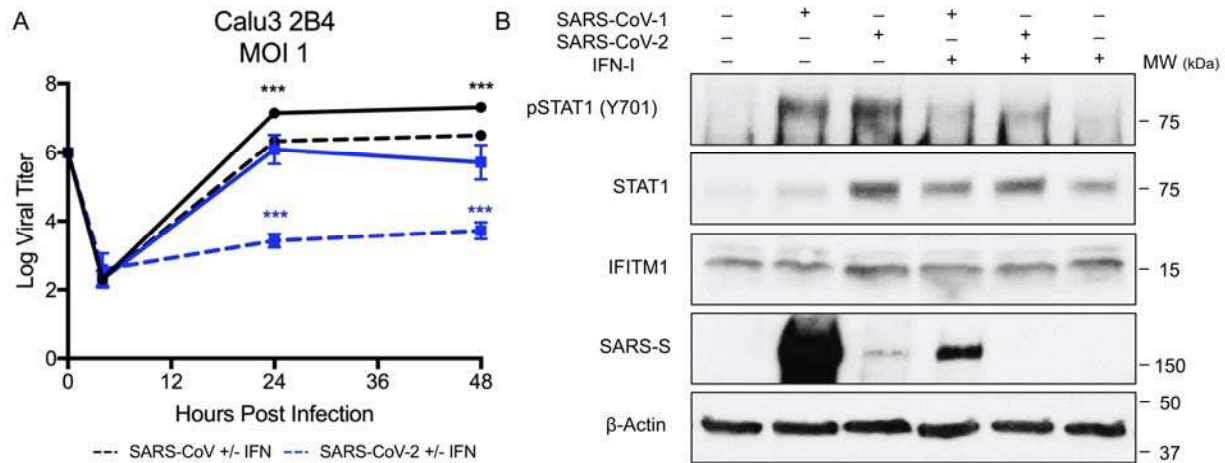
643

644

Figure 1. SARS-CoV-2 sensitive to type I IFN pretreatment. A) Vero E6 cells were treated with 1000 U/mL recombinant type I (hashed line) IFN or mock (solid line) for 18 hours prior to infection. Cells were subsequently infected with either SARS-CoV WT (black) or SARS-CoV-2 (blue) at an MOI of 0.01 as described above. Each point on the line graph represents the group mean, N ≥ 3. All error bars represent SD. The two tailed student's t-test was used to determine P-values: *** $P < 0.001$. B) Vero cell protein lysates from IFN-I treated and untreated cells were probed 48 hours post infection by Western blotting for phosphorylated STAT1 (Y701), STAT1, IFITM1, SARS spike, and Actin.
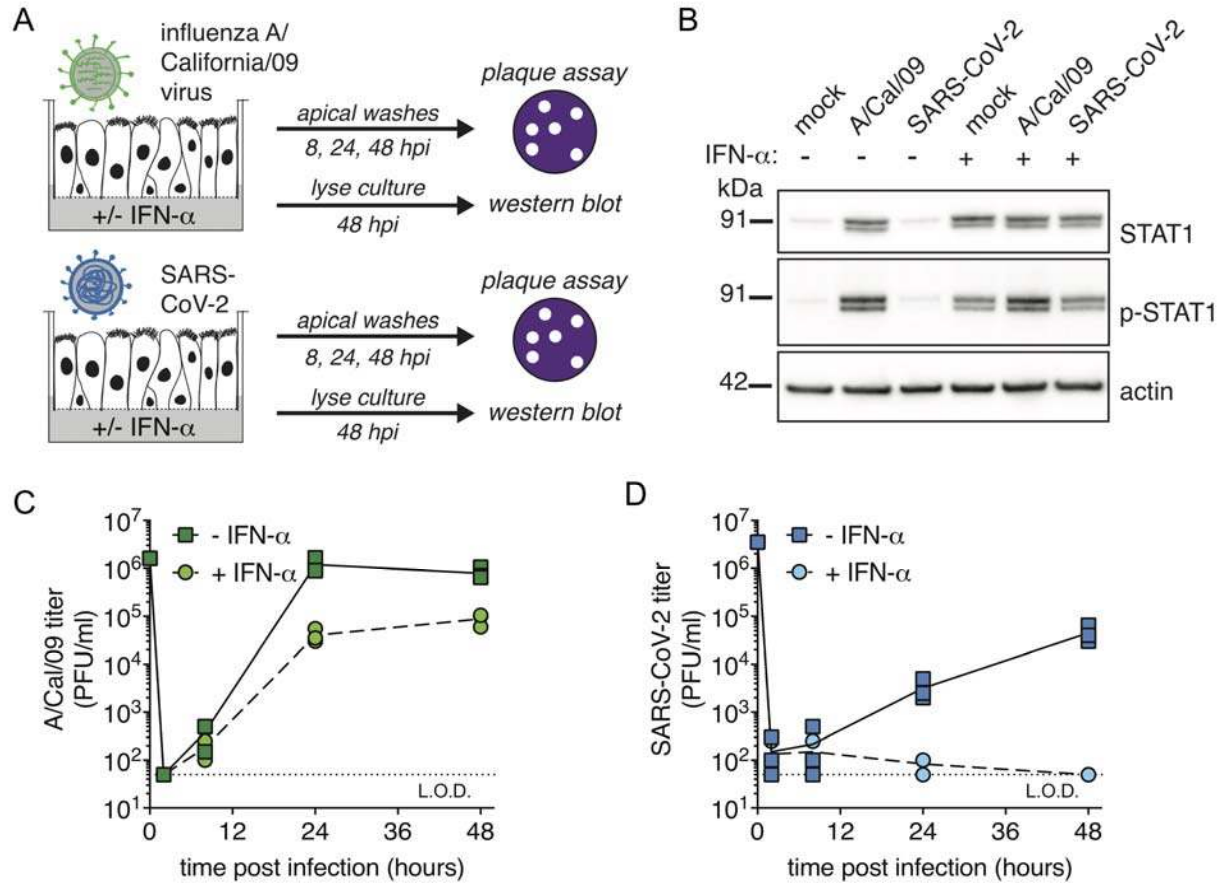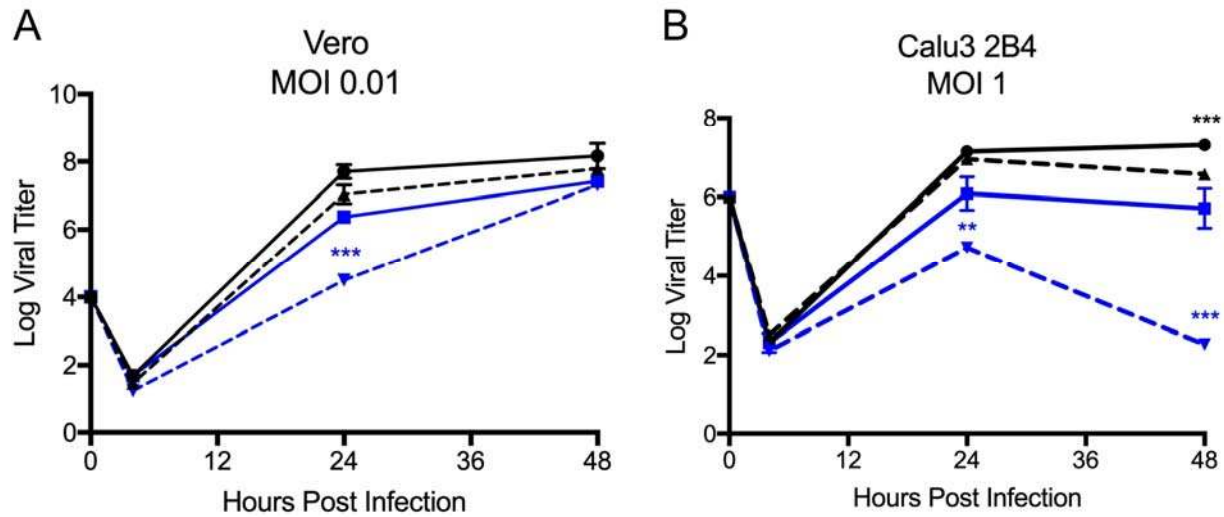
653

654

655
656

657 **Figure 2. SARS-CoV-2 attenuated and IFN-I sensitive in Calu3 respiratory cells**. A) Calu3
658 2B4 cells were treated with 1000 U/mL recombinant type I (hashed line) IFN or mock (solid line)
659 for 18 hours prior to infection. Cells were subsequently infected with either SARS-CoV WT
660 (black) or SARS-CoV-2 (blue) at an MOI of 1. Each point on the line graph represents the
661 group mean, N ≥ 3. All error bars represent SD. The two tailed student's t-test was used to
662 determine P-values: *** P < 0.001. B) Calu3 cell protein lysates from IFN-I treated and untreated
663 cells were probed 48 hours post infection by Western blotting for phosphorylated STAT1 (Y701),
664 STAT1, IFITM1, SARS spike, and Actin.

665

666
667

Figure 3. Differential IFN-I sensitivity and pSTAT1 phosphorylation following SARS-CoV-2 or influenza A virus on polarized human airway epithelial cultures (HAEC). A) HAEC were pretreated with 1000 U/mL IFN-α basolaterally for 2 hours prior to and during infection. Cultures were then infected apically with influenza A/California/09 H1N1 virus or SARS-CoV-2. Apical washes were collected at the indicated times and progeny titers determined by plaque assay on MDCK cells (influenza virus) or Vero E6 cells (SARS-CoV-2). At the 48 h endpoint, cultures were lysed for western blot analysis. B) Western for total STAT1 or phospho-STAT1 at 48 hpi. C) Influenza A virus titers by plaque assay on MDCK cells. 0 h, virus inoculate; 2 h, virus in third apical wash; 8, 24, 48 h, virus in apical washes at these time points. D) SARS-CoV-2 titers by plaque assay on Vero E6 cells. 0 h, virus inoculate; 2 h, virus in second apical wash; 8, 24, 48 h, virus in apical washes at these time points.

679

680

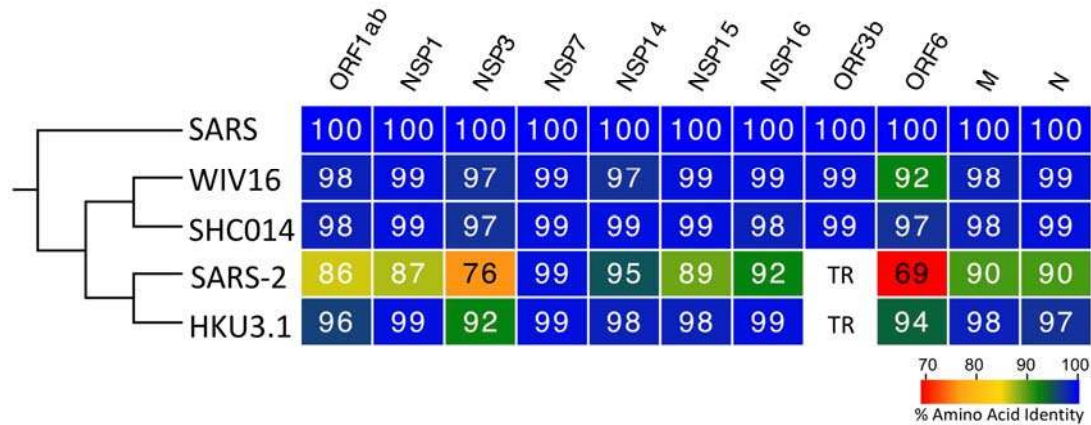**Figure 4, SARS-CoV-2 impacted by post IFN-I treatment**. A-B) Vero E6 and Calu3 2B4 cells were infected with either SARS-CoV WT (black) or SARS-CoV-2 (blue) at an MOI 0.01 (A, Vero cells) or MOI 1 (B, Calu3 cells). Cells were subsequently treated with 1000 U/mL recombinant type I IFN (hashed line) or mock (solid line) for 4 hours following infection. Each point on the line graph represents the group mean, N ≥ 3. All error bars represent SD. The two tailed student's t-test was used to determine P-values: **P <0.01 *** P < 0.001.

687

Figure 5, Conservation of SARS-CoV IFN antagonists. Viral protein sequences of the indicated viruses were aligned according to the bounds of the SARS-CoV open reading frames for each viral protein. Sequence identities were extracted from the alignments for each viral protein, and a heat map of percent sequence identity was constructed using EvolView (www.evolgenius.info/evolview) with SARS-CoV as the reference sequence. TR = truncated protein.